

**An NBS Calibration Procedure for Providing Time and
Frequency at a Remote Site by Weighting and Smoothing
of GPS Common View Data**

M.A. Weiss

D.W. Allan

**Reprinted from
IEEE TRANSACTIONS ON INSTRUMENTATION AND MEASUREMENT
Vol. IM-36, No. 2, June 1987**

An NBS Calibration Procedure for Providing Time and Frequency at a Remote Site by Weighting and Smoothing of GPS Common View Data

MARC A. WEISS AND DAVID W. ALLAN

Abstract—The National Bureau of Standards (NBS) Time and Frequency Division now performs precision time and frequency transfer using common view measurements of Global Positioning System (GPS) satellites as a calibration service. Using this service, we have been able to transfer time with time stabilities of a few nanoseconds, time accuracies of the order of 10 ns, and frequency stabilities of one part in 10^{14} , or better, for measurement times of about four days and longer. The full accuracy of the NBS primary frequency standard is now available at a remote site. This paper describes the technique used for weighting and smoothing the data to produce these levels of stability and accuracy. All of the primary frequency standards used in the generation of International Atomic Time (TAI) now use this technique.

I. INTRODUCTION

IT IS NOW possible to compare a clock with universal time coordinated (UTC(NBS)) anywhere in common view of a Global Positioning System (GPS) satellite with Boulder, CO at the full level of accuracy and stability of the National Bureau of Standards (NBS) atomic time scale for integration times of about four days and longer via the NBS Global Time Service. This availability includes East Asia, Europe, and North, Central, and South America. The service includes a dial-up line to one of the NBS computers for current estimates for the user's clock performance, and a monthly report for improved estimates after the fact. We discuss here the method by which the common view time transfer values in the monthly reports are computed.

There are several important aspects to the method NBS uses in obtaining state-of-the-art time transfer: making the measurements and checking the data for outliers, characterizing the random and systematic variations in the data, determining nominal optimum weights for the data, and Kalman smoothing the weighted averages and interpreting the results. First, simultaneous measurements are taken using a satellite in common view of NBS Boulder and a second location. These measurements are repeated each sidereal day so that the geometry at measurement time remains fixed. The data are checked for statistical outliers, and these are removed by interpolation or extrapolation. Second, we characterize the random and systematic variations. A measurement geometry which re-

peats each sidereal day defines a time series for each of the common view GPS satellites employed. The type of measurement noise and the noise level of each time series is determined using a decomposition of variances from independent satellite comparisons. The noise type is determined initially in defining the model, and should stay the same unless something in the system changes. The level of the noise is determined independently for each monthly report. Also, a comparison of the biases between pairs of comparisons can be checked. Third, a nominally optimum set of weighting factors can be calculated knowing the noise levels. These are used to combine the measurements via different satellites into a single weighted average. Fourth, a Kalman smoothed estimate of time and fractional frequency offset of the remote clock is separately computed for each time series, using the measurement noise estimates along with the noise characteristics of the clocks involved; and finally, these are also combined using the weights previously determined to define optimal estimates of time and frequency offsets of the remote clock.

Using the above technique we have been able to transfer time with a standard deviation on the measurement noise residuals of the order of 1 ns and with time accuracies of the order of 10 ns.

II. DATA SELECTION AND REJECTION

Locations interested in comparing a clock with UTC(NBS) via GPS should measure their clock against GPS satellites according to an NBS tracking schedule. Recently NBS in support of the Bureau International de l'Heure (BIH), has transferred the technique for developing this tracking schedule to the BIH. A satellite is tracked for a 13-min interval and the data taken during that time are reduced to a value of GPS minus reference clock and a rate offset. It has been shown elsewhere [1] that tracking longer than about 10 min is of little value since the fluctuations appear to be flicker noise phase modulation (PM) limited for Fourier frequencies smaller than about one cycle per 10 min. One gains significantly by averaging the white phase noise at the higher Fourier frequencies. Tracks are extended to 13 min to ensure use of the most recent ionospheric correction, since that parameter is transmitted every 12.5 min. The tracking

Manuscript received June 23, 1986.

The authors are with the Time and Frequency Division, National Bureau of Standards, Boulder, CO 80303.

IEEE Log Number 8613610.

schedule tells which satellites to track at what time on a certain modified Julian day (MJD) for all locations in a given large area of earth. Each track in the tracking schedule is assigned to at least two areas and is chosen to maximize the elevation of a GPS satellite as seen from those areas. The elevation of a satellite changes little over a large area of earth since the satellite orbits are 4.2 earth radii. The track times decrement by 4 min a day to preserve the geometric relationship between the satellites and the ground location at each measurement. This follows since the satellites are in 12-h sidereal orbits. A sidereal day is not exactly 4 min less than a solar day, but this is close enough since the satellites deviate somewhat from exact sidereal orbits. The tracking schedule is recomputed from time to time (about once or twice a year) in order to maintain good geometry.

GPS minus reference measurements are gathered together at NBS in Boulder from many locations in the United States and around the world. UTC(NBS) can be transferred to any location having common view data with NBS. A track is in common view between two locations if both locations have received the same signals from a satellite, i.e., both locations have tracked the same satellite at the same time. In this way many sources of error cancel or nearly cancel upon subtraction of the GPS minus reference measurements [2]. If there is some discrepancy between the times of tracking at the two locations the noise of the difference measurement may degrade. A common view track repeats every sidereal day and in this way defines a time series comparing the clocks at the two locations. Each time series represents a different path from one location to the satellite to the other location repeated every sidereal day and used to compare the two reference clocks. Each satellite in common view can be used for such a time series. Indeed, a satellite can give rise to two time series if there are two different common view paths each day: one when the satellite is nominally between the two locations, and one about 12 h later when observed over the pole. Time transfer between two locations is accomplished by determining measurement noise and weights for each path, using this to smooth each time series separately and combine them into a weighted average.

We often find that the entire time series of common view measurements via one satellite is biased from the data via another satellite. This is not entirely understood, but it must be due either to repeated errors in the transmitted ephemeris or ionospheric model, or repeated errors in the tropospheric model, coordinate errors at the local receiver, or a frequency offset between the reference clocks. Because of these biases, we work with the time series separately before they are combined into a weighted average. Also, the presence of the biases makes choosing the weights very important since the resultant average can change with different weights. First, each time series is studied for apparent bad points. These may be due to a reference clock time or frequency step, in which case points in the time series may seem bad but are actual mea-

surements of the clock. If this happens when there are missing data from several satellites it can be difficult to interpret. Bad points can also be caused by either troubles in the data transmitted from the satellite or problems in the receiver. A knowledge of clock characteristics and experience with the GPS performance is necessary in order to make proper judgements in dealing with any of the above bad points. When these are found in a given time series—and they are not attributable to the reference clock—they are replaced by a value either linearly interpolated from neighboring good points, or, if it is an end point, by a value extrapolated from the entire time series by a quadratic curve fit. In this way a bad measurement is replaced with a value which maintains the bias of the time series when it is included in the weighted average. Extrapolated data have to be used very cautiously.

III. MEASUREMENT NOISE AND WEIGHTS

The measurement noise and the weight of each time series is estimated using a decomposition of variance or what is called an “*N*-corner hat” technique with the modified Allan variance. The *N*-corner hat technique is a generalization of the three-corner hat [3], where the variance of the stability of a particular clock is estimated using variances of the stability of difference measurements among three clocks. The generalization is that we have *N* clocks instead of three. We apply this technique to differences of the time differences of our GPS data, i.e., differencing the common view measurements across satellites. The equations are as follows. A time difference is a difference of measurements at two locations via satellite *i*:

$$\begin{aligned} (\text{Ref}_2 - \text{Ref}_1 + \text{Noise})_i &= (\text{GPS} - \text{Ref}_1 + \text{Noise})_i \\ &\quad - (\text{GPS} - \text{Ref}_2 + \text{Noise})_i \end{aligned}$$

where “Noise” on the left denotes the common view measurement noise for that path.

The difference of the differences is

$$\begin{aligned} \text{Noise}_i - \text{Noise}_j &= (\text{Ref}_2 - \text{Ref}_1 + \text{Noise})_i \\ &\quad - (\text{Ref}_2 - \text{Ref}_1 + \text{Noise})_j. \end{aligned}$$

Thus we see that the set of variances of the difference of differences is the set of variances of noise differences. We may apply *N*-corner hat to this to find the variance of a particular process just as we apply *N*-corner hat to the set of variances of clock stability differences to find the stability of a particular clock. Let us consider the equations for the composition of variances [4]. We want to find

$$\sigma_i^2 = \text{estimate of the variance of process } i,$$

$$i = 1, 2, \dots, N$$

given

$$s_{ij}^2 = \text{measurement of the variance of } i - j \text{ difference}$$

and under the assumption that the common view noise via satellite *i* is uncorrelated with that via *j*.

We choose the σ_i^2 to minimize

$$A = \sum_{j=2}^N \sum_{i=1}^{j-1} (s_{ij}^2 - \sigma_i^2 - \sigma_j^2)^2.$$

The result after solving $\partial A / \partial \sigma_i^2 = 0$ is

$$\sigma_i^2 = \frac{1}{N-2} \left(\sum_{k=1}^N s_{ik}^2 - B \right)$$

where

$$B = \frac{1}{2(N-1)} \left(\sum_{k=1}^N \sum_{j=1}^N s_{kj}^2 \right), \quad \text{with } s_{jj}^2 = 0.$$

If we use the modified Allan variance [5], [6] in these equations we see that the common view noise has a spectrum consistent with the hypothesis of white noise PM. This means that the square root of the variance as a function of time interval τ should be proportional to $\tau^{-3/2}$, or where $\tau = m\tau_o$ (m is an integer and τ_o is one sidereal day). Because of this we may multiply $\sigma_i^2(m \cdot \tau_o)$ by m^3 and take the mean over the number M of variance computations. Thus the common view noise squared n_i^2 for path i is proportional to

$$n_i^2 \sim \frac{1}{M} \sum_{k=0}^{M-1} [\sigma_i^2(2^k \tau_o) * (2^k)^3].$$

The constant of proportionality is

$$\tau_o^2/3p_i, \quad \text{where } p_i \text{ is the percentage of good points.}$$

The factor of $\tau_o^2/3$ comes from the relationship between time and frequency stability with the modified Allan variance in the case of white noise PM (see Appendix). The percentage of good points comes in because the confidence of the estimate gets worse with fewer points [7]. The weight of path i , w_i , is the reciprocal of the normalized noise estimate of path i , w_i , is the reciprocal of the normalized noise estimate

$$w_i = (1/n_i^2) / \left(\sum_j 1/n_j^2 \right).$$

These are the weights which are used to combine the time series for the different satellite paths into a single weighted average. The result is that the more stable the series, the heavier it is weighted. This is optimum for unbiased data. If the bias of a path is proportional to its instability, then the weighted average will also be optimum. There are some mechanisms in the GPS that make this a good assumption. If a bias is due to local coordinate errors this assumption will fail. Biases due to coordinate errors are estimated to be only a few nanoseconds if the coordinates used are self-consistent with the GPS. Biases of several nanoseconds can occur if an independent coordinate determination is used. If the bias is due to error in transmitted data it is possible the bias would be unstable from attempts to correct the error and the above assumption would be valid. A study is in progress to better understand these biases. Despite the biases, this optimum weighting procedure leads to minimum measurement

noise for frequency calibration and frequency transfer at a remote site.

The above procedure does not consider weighting due to the confidence of the estimate as that has not been developed yet for the modified Allan variance. For the Allan variance and the case of white noise PM it has been shown that the confidence of the estimate remains fairly constant [8]. It is believed that a similar result will be true for the modified Allan variance in which case the above equations are properly weighted.

IV. KALMAN ESTIMATES

Once the measurement noise level and type are characterized, a forward-backward Kalman smoother is designed and used to optimize the signal to noise for time and frequency transfer. Each path is smoothed separately using the estimates of the noise for each path, as well as estimates for the noise characteristics of the two clocks, as input to the Kalman smoother. The state vector consists of two elements: the time x and fractional frequency y of a clock offset from UTC(NBS). Interpolated or extrapolated values are not used by the Kalman, rather it replaces these with its own optimal estimates. The x and y values from the different paths are combined using the weights to generate a smoothed estimate of the time and frequency offset of a reference clock from UTC(NBS).

V. RESULTS

Results of approximately 10-ns accuracy and 1 part in 10^{14} stability for integration times of four days have been reported elsewhere [9]. Here we simply note results on more recent data. We consider time comparisons between NBS in Boulder, CO, and Physikalisch-Technische Bundesanstalt (PTB) in Braunschweig, West Germany during a 94-day period from MJD 46490 to 46583, March 1 to June 2, 1986. We use measurements via paths for six satellite vehicles (SV's), SV 3, SV 8, SV 9, SV 11, SV 12, and SV 13. The raw data can be seen in Fig. 1(a) and 1(b) via each of these paths. The biases between the paths can be seen here. To reveal the biases more clearly we compute the differences of common view paths of satellites measured against each other. These differences of differences are the input to the six-corner hat. The mod $\sigma_y(\tau)$ values from the six-corner hat for SV 3 are shown in Table I. This illustrates agreement with the $-3/2$ slope for the white phase modulation model.

Now compare this with the $\sigma_y(\tau)$ values for the time transfer shown in Table II. We see that the measurement noise may yet be present at one or two days of integration, but quickly drops below the noise of the clocks for periods of four days or greater.

Table III tabulates the average biases for each track against a weighted mean and the computed measurement noise for each of the satellite paths. We look at Table III to consider our hypothesis that a larger bias is associated with a larger measurement noise. The worst measurement noise values are for SV's 3, 9, and 11. These are all biased

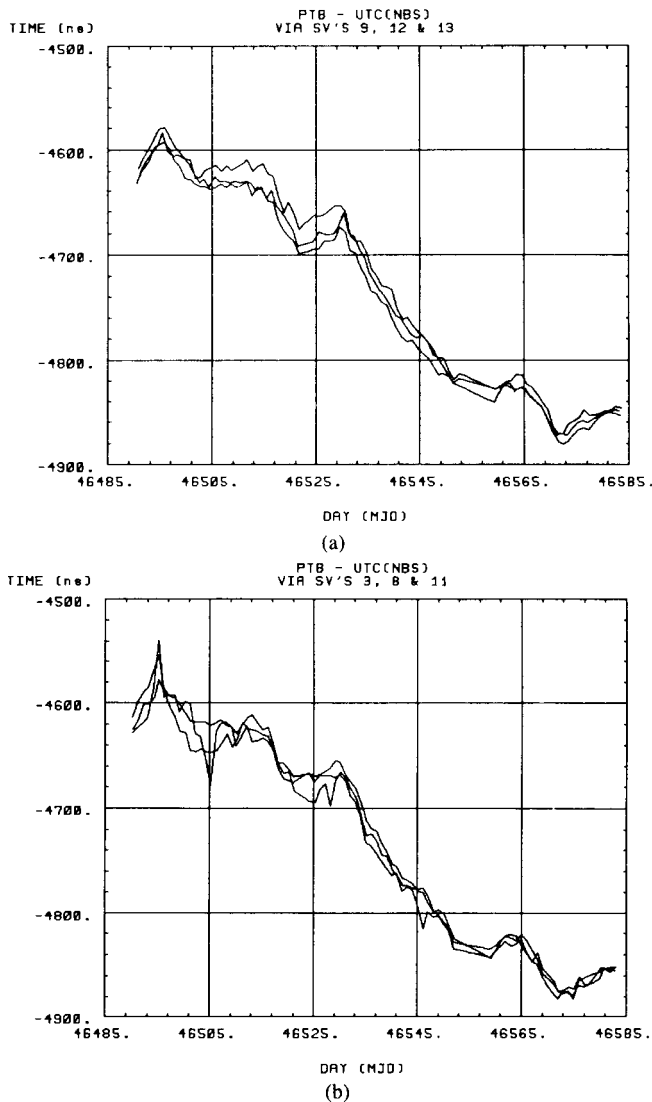


Fig. 1. (a) A plot of the time difference between UTC(PTB) and UTC(NBS) via three GPS satellites (NAVSTAR's 6, 10, and 9, respectively, for the Space Vehicle numbers in the heading) used in common view. (Peak-to-peak bias of up to about 20 ns can be observed. The baseline is 8050 km. The consistency of observing the relative time scale deviations via any one of the three common view estimates is also apparent.) (b) This plot is similar to (a) (The NAVSTAR satellites chosen in this case were 11, 4, and 8, respectively, for the space vehicle numbers in the heading. The biases and scatter are noticeably larger over the first part of the 94-day interval. A weighted average and smoothing will clearly be beneficial.)

do know that for time stability and frequency accuracy we are optimally weighting the data.

the same way, though the values are quite different. The smaller measurement noise values for SV's 8, 12, and 13 seem to go with smaller biases, but the results are marginal. We simply do not know the right answer here for time accuracy. We believe that since each common view path should be an independent estimate, the standard deviation should be a good measure of the accuracy. It is not certain that the biases are independent. In fact, in some cases there are mechanisms for dependency between some of the biases. They can occur through the Kalman estimation process, for example. More study is needed. We

TABLE I
COMMON-VIEW MEASUREMENT STABILITY FOR SV3 BETWEEN PTB AND NBS FROM THE SIX-CORNER HAT TECHNIQUE

τ in sidereal days	$\sigma_y(\tau)$
1	14.7 E-14
2	7.3 E-14
4	3.3 E-14
8	0.9 E-14
16	0.4 E-14

TABLE II
STABILITY OF PTB CLOCK VERSUS NBS CLOCK VIA THE COMMON-VIEW WEIGHTED-ESTIMATE

τ in sidereal days	$\sigma_y(\tau)$
1	5.3 E-14
2	4.4 E-14
4	4.4 E-14
8	2.4 E-14
16	1.9 E-14

TABLE III
COMPARISON OF COMMON-VIEW BIASES AND MEASUREMENT NOISE VALUES

SV #	Average Bias vs. weighted mean	Meas.Noise (ns)
3	- 5.6	12.2
8	+ 3.1	5.8
9	- 9.7	11.2
11	- 5.1	11.9
12	+ 5.1	6.2
13	- 4.1	7.6
Standard Deviation about the weighted mean		Composite Meas. Noise
6.4		3.2

The rms standard deviation of the different SV paths averaged over the 94 days is 9.2 ns. This is due primarily to the biases, since the composite measurement noise is only 3.2 ns. The latter is an indication of the measurement noise remaining in the weighted average. The weighted average for the time transfer across the satellites is in Fig. 2. The $\sigma_y(\tau)$ for these data is plotted in Fig. 3. Knowing something about the clocks involved we see there can be little remaining measurement noise. We attempt to remove this with a Kalman Smoother. Fig. 4 shows the time residuals for UTC(PTB) - UTC(NBS) after the smoother, and Fig. 5 shows the associated $\sigma_y(\tau)$.

A good check of the consistency of the time transfer system via GPS in common view is to perform time transfer around the world using several different reference stations. In Fig. 6 we see the results of this using NBS, PTB, and the Tokyo Astronomical Observatory (TAO) in To-

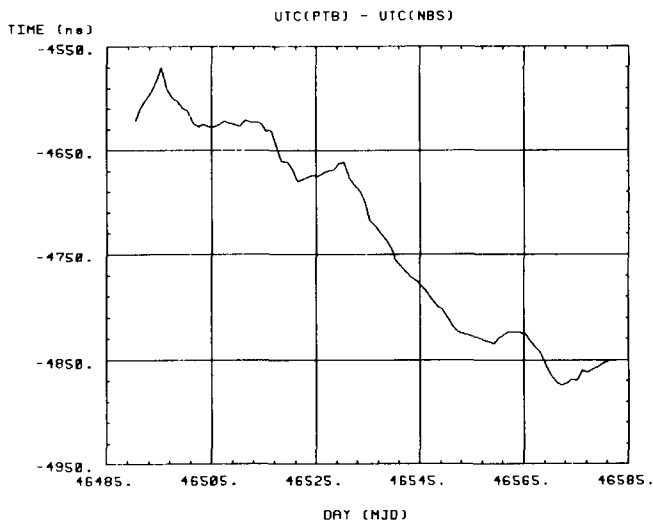


Fig. 2. A plot of the weighted average of the time difference of UTC(PTB) - UTC(NBS). (The rms standard deviation about the weighted mean over the 94 days was 9.2 ns. The white noise PM was estimated to be 3.2 ns. The difference between these two numbers is primarily due to the biases in the system.)

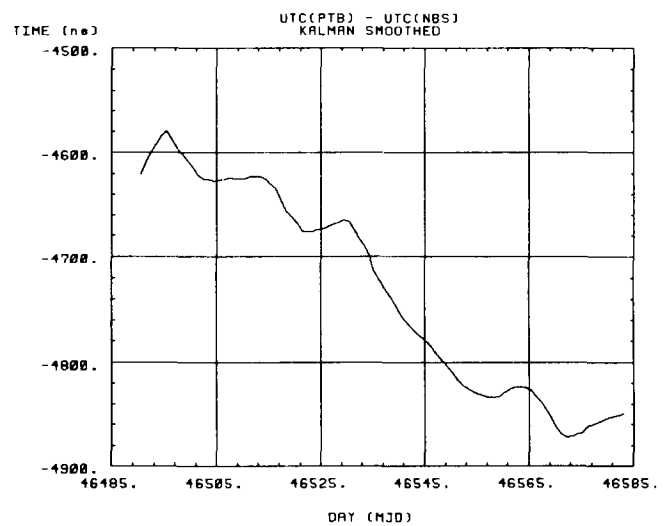


Fig. 4. A plot of the Kalman smoothed GPS common view time difference between the PTB and NBS time scales. (Choosing the appropriate Kalman parameters reduces the GPS common view noise contribution so that all values are more nearly representative of the time scales involved.)

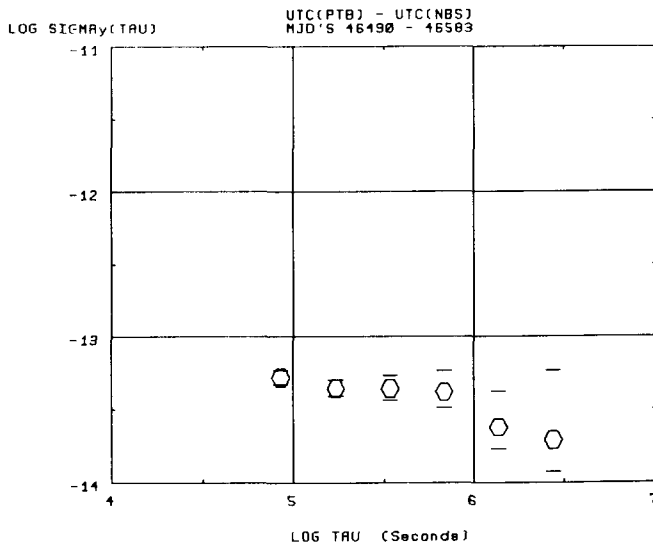


Fig. 3. The fractional frequency stability (square root of the two sample or Allan variance) as a function of the sample time τ is plotted using the data shown in Fig. 2. (The GPS common view noise contributes to the instabilities plotted an estimated amount of $\sigma_y(\tau) = 6.4 \text{ E-}14/\tau$, where τ in this equation is in units of days. The sample times plotted are for $\tau = 1, 2, 4, 8, 16,$ and 32 days. Hence, the common view noise only contaminates somewhat the time scale comparison stability for $\tau = 1$ and 2 days.)

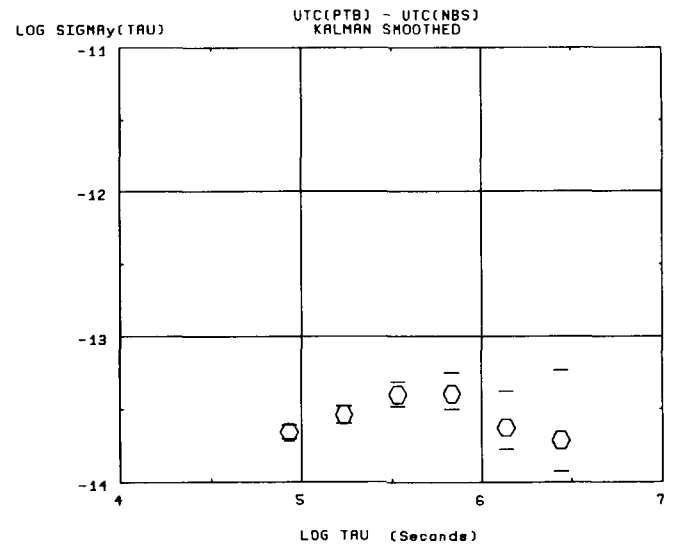


Fig. 5. A plot of $\sigma_y(\tau)$ for the data shown in Fig. 4. (If the Kalman smoothing parameters are well chosen and the models appropriate to the clocks' stochastic processes, the fractional frequency stabilities plotted will be good estimates of the relative time scale stabilities even over the 8050-km baseline between the scales.)

kyo, Japan over a period of 569 days from MJD 46014 to 46582, November 10, 1984 to June 1, 1986. We see that the values stay biased away from zero for long periods of time. Here we see clearly the effect of the biases on time accuracy.

An example of a state-of-the-art time and frequency transfer experiment is illustrated in Figs. 7 and 8, which is a time and frequency stability comparison of the National Research Council (NRC), Ottawa, Canada, primary cesium clock and the NBS prototype passive hydrogen maser utilizing the above outlined technique via seven

independent GPS satellite clocks. The theoretical noise estimated from the N -corner hat analysis is plotted along with the theoretical white frequency modulation noise from the NRC primary cesium and from the passive maser for comparison with the measured values. The excellent agreement is apparent.

In addition to using this service for the above-mentioned Global Time Service, it is used in computing the data sent to the BIH for the NBS input of the Système International d'Unités (SI) second and for the input of the times of the clocks in the NBS ensemble toward the generation of UTC and TAI. These data include comparisons of the time and frequency of UTC(NBS) with other principal timing centers, e.g., the NRC, PTB, the Radio Re-

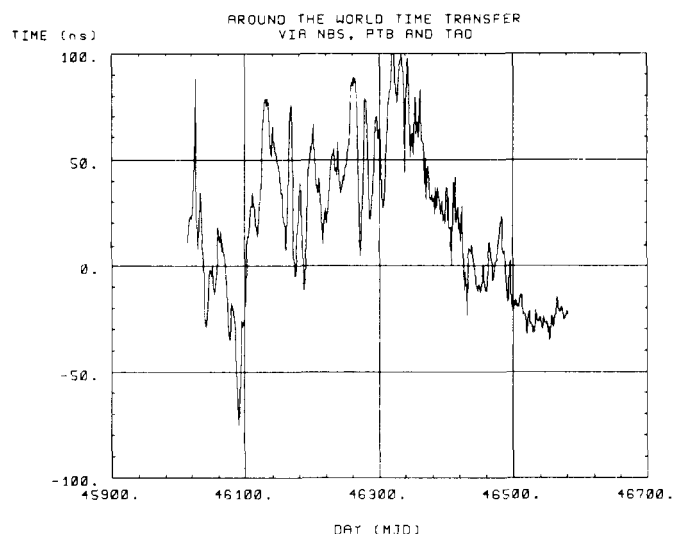


Fig. 6. A plot of the consistency and the accuracy of the GPS common view approach over some nearly 600 days of data. (The errors plotted are the accumulation over three GPS common view paths: PTB-NBS, TAO-PTB and NBS-TAO, which would add to zero if the technique were perfect. There are clearly biases in the system of the order of several tens of nanoseconds, which walk in and out with time. Dividing the accumulated bias by three gives one common view comparison an accuracy of the order of 10 ns over the last several months. Whether that persists or not remains to be seen. Further understanding of these biases is needed.)

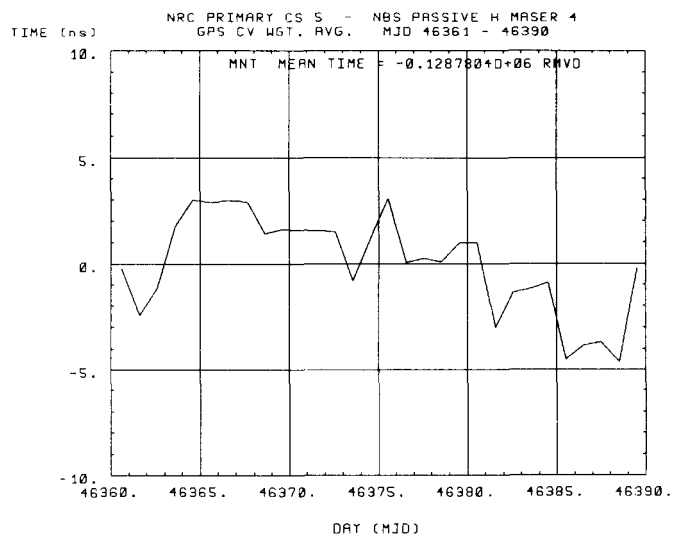


Fig. 7. A plot of the time difference residuals between the NRC primary cesium clock, Cs 5, and the NBS prototype passive hydrogen maser, PHM4 as measured via the weighted filtered average of seven GPS satellites utilized in the NBS-GPS common view time transfer mode. (MID RMVD means the mean frequency was removed from the data by subtracting a mean first difference from the weighted average difference data. A mean time was removed (MNT: RMVD) for scaling convenience.)

search Laboratory (RLL) in Tokyo, and the U.S. Naval Observatory in Washington DC. The above technique was utilized in making a comparison across the Pacific of the NBS and RLL primary frequency standards. This is the first time (October–November 1984) they had been compared where their full accuracy was appreciated. The RLL primary standard Cs 1 was compared with the NBS primary standard NBS-6; the fractional frequency difference

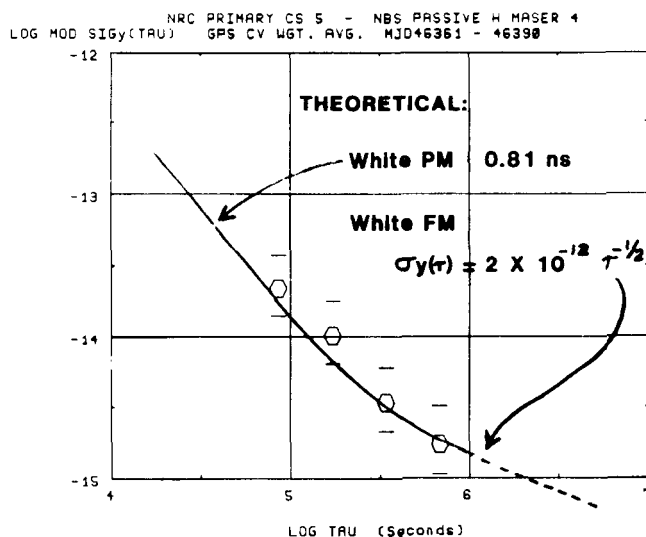


Fig. 8. A plot of the square root of the modified Allan variance of the weighted average of the data, but before filtering. (The instabilities are composite from the two clocks involved, the two NBS-GPS common view receivers, and the weighted average common view noise. NAVSTAR's 3, 4, 6, 8, 9, 10, and 11 were employed. The actual instabilities measured are consistent with a white noise phase modulation for the measurement noise of 0.8 ns and a white noise frequency modulation for a clocks of $\sigma_y(\tau) = 7 \times 10^{-15} \tau^{-1/2}$, where τ is in days and with τ ranging from of 1 to 8 days.)

was measured to be

$$Cs\ 1 - NBS-6 = (2 \pm 14) \times 10^{-14}.$$

The difference is, interestingly, about nine times smaller than the gravitational "red shift" that had to be applied in making the comparison.

VI. CONCLUSIONS

Time transfer via GPS satellites is possible at the level of accuracy of laboratory time standards for periods of four days or more, depending on the baseline and if it is done with care. Care is needed in making strictly simultaneous measurements at two locations repeated every sidereal day to maintain a common view measurement with a constant geometry. Care is needed in removing bad points from each of the time series. Weights for each path are very important since, due to biases in the system, a change in weights significantly changes the weighted mean. Finally, a Kalman smoother may be employed to remove measurement noise from the weighted average, but its results must be interpreted carefully. Understanding the biases in the system remains an important unsolved problem.

APPENDIX

CLASSICAL OR N-SAMPLE VARIANCE VERSUS $\sigma_y^2(\tau)$, THE TWO-SAMPLE OR ALLAN VARIANCE

We will derive the relationship between the classical phase variance and the Allan variance. The ratio of expected value of the classical or N-point fractional frequency variance to the Allan variance has been derived for an arbitrary power law spectrum μ , and as a function of N, the number of data samples, T the period of sam-

pling, and τ the sample time [10], [11]. Let us denote the expected value of the N -sample fractional frequency variance with $T = \tau$ (no dead time) as

$$\langle \sigma_y^2(N, \tau) \rangle.$$

Then if we denote the ratio

$$B_1(N, \mu) = \frac{\langle \sigma_y^2(N, \tau) \rangle}{\sigma_y^2(\tau)}$$

it can be shown from results in [10], [11] that

$$B_1(N, \mu) = \frac{N(N^\mu - 1)}{2(N - 1)(2^\mu - 1)}.$$

For white phase noise we have $\mu = -2$. Hence as N grows large without bound we have

$$B_1(N, \mu) \rightarrow 2/3, \quad \text{as } N \rightarrow \infty, \mu = -2.$$

To complete our derivation we will show the relationship between the classical fractional frequency variance and the classical phase variance. Since the phase variations are proportional to the time variations ($x = \phi/2\pi\nu_0$), the relationship between fractional frequency y and time x is

$$y(t) = \frac{x(t + \tau) - x(t)}{\tau}.$$

If we compute a classical variance of both sides, and if the phase points $x(t)$ are consistent with a white phase noise model so $x(t + \tau)$ and $x(t)$ are uncorrelated, we have as the number of samples N approaches ∞

$$\begin{aligned} \sigma_y^2(N \rightarrow \infty, \tau) &= \frac{\sigma_x^2(N \rightarrow \infty, \tau)}{\tau^2} \\ &+ \frac{\sigma_x^2(N \rightarrow \infty, \tau)}{\tau^2} = \frac{2}{\tau^2} \sigma_x^2(\tau). \end{aligned}$$

If we substitute this into our result above

$$\frac{\langle \sigma_y^2(N \rightarrow \infty, \tau) \rangle}{\sigma_y^2(\tau)} = \frac{2}{3}$$

we have

$$\frac{2\sigma_x^2(\tau)}{\tau^2\sigma_y^2(\tau)} = \frac{2}{3}$$

hence

$$\sigma_x^2(\tau) = \frac{\sigma_y^2(\tau) \cdot \tau^2}{3}.$$

REFERENCES

- [1] D. D. Davis, M. A. Weiss, A. C. Clements, and D. W. Allan, "Remote synchronization within a few nanoseconds by simultaneous viewing of the 1.575 GHz GPS satellite signals," W. J. Alspach, Ed., *CPEM Dig.*, p. N15, 1982.
- [2] D. W. Allan and M. A. Weiss, "Accurate time and frequency during common-view of a GPS satellite," in *Proc. 34th Annu. Symp. Frequency Control* (Fort Monmouth, NJ), 1980, p. 334.
- [3] J. E. Gray and D. W. Allan, "A method for estimating the frequency stability of an individual oscillator, in *Proc. 28th Annu. Symp. Frequency Control*, May 1974, pp. 243-246.
- [4] J. A. Barnes, "Time scale algorithms using Kalman filters—Insights from simulation," in *Proc. 2nd Symp. Time Scale Algorithms*, NBS, (Boulder, CO), June 23-25 1982, app. C.
- [5] D. W. Allan and J. A. Barnes, "A modified 'Allan Variance' with increased oscillator characterization ability," in *Proc. 35th Annu. Symp. Frequency Control* (Fort Monmouth, NJ), 1981, p. 470.
- [6] P. LeSage, "Characterization of frequency stability: Analysis of the modified Allan variance and properties of its estimate," *IEEE Trans. Instrum. Meas.*, vol. IM-33, pp. 332-336, 1984.
- [7] P. LeSage and C. Audoin, "Characterization of frequency stability: Uncertainty due to the finite number of measurements," *IEEE Trans. Instrum. Meas.*, vol. IM-22, no. 2, June 1973.
- [8] D. A. Howe, D. W. Allan, and J. A. Barnes, "Properties of signal sources and measurement methods," in *Proc. 35th Ann. Freq. Control Symp.*, 1981, pp. 669-715.
- [9] D. W. Allan *et al.*, "Accuracy of international time and frequency comparisons via global positioning system satellites in common-view," *IEEE Trans. Instrum. Meas.*, vol. IM-34, no. 2, p. 118, June 1985.
- [10] D. W. Allan, "Statistics of atomic frequency standards," *Proc. IEEE*, vol. 54, 1966.
- [11] J. A. Barnes, "Tables of bias functions, B_1 and B_2 , for variances based on finite samples of processes with power law spectral densities," Nat. Bur. Stand. Tech. Note 375, Jan. 1969.